crystals

MDPI

Article

Structural Comparison of Three *N*-(4-Methoxyphenyl)-Nitrobenzenesulfonamide Derivatives

Mark Oblazny and Christhoper G. Hamaker *

Department of Chemistry, Illinois State University, Normal, IL 61790-4160, USA
* Correspondence: chamaker@illinoisstate.edu; Tel.: +1-309-438-7659

Abstract

The series of all three *N*-(4-methoxyphenyl)-nitrobenzenesulfonamides has been synthesized and their crystal structures analyzed. The bond lengths and angles are all very similar, only the C-S-N-C torsion angles are significantly different in the three molecules, leading to different orientations of the phenyl rings in the molecules. All three molecules exhibit N–H···O hydrogen bonds with the sulfonamide group; however, in only two of the three is the acceptor an oxygen atom on the sulfonamide group. In the third, the acceptor oxygen is the methoxy oxygen atom. Compound **A** forms an infinite three-dimensional network, compound **B** exhibits ladder-shaped sheets, and **C** shows infinite sheets that are fairly planar. Overall, the differences in overall intermolecular interactions appear to be driven by packing rather than by the overall shapes of the molecules themselves.

Keywords: sulfonamides; hydrogen bonding; crystal structure; structure variation; noncovalent interactions; Hirshfeld surface

1. Introduction

Sulfonamides were first recognized as potential drugs in the early 1930s when Gerhard Domagk tested Prontosil, a sulfonamide azo dye, as a treatment for bacterial infections [1]. Domagk received the 1939 Nobel prize in Medicine for his discovery. While sulfonamide drugs were once among the most common, today there are only about 40 FDA approved sulfonamide drugs [2]. Recently, however, attention has turned back to sulfonamides as drug candidates due to their many favorable characteristics, including biocompatibility [3] and ease of synthesis [4]. Currently, several sulfonamides are being studied as anti-cancer agents [5,6]. A recent study identified several sulfonamide molecules that act as inhibitors of Lemur tyrosine kinase 3, several at sub-micromolar concentrations [7]. Lemur tyrosine kinase 3 has been shown to promote tumor development by numerous pathways [8]. Additionally, sulfonamides have also been shown to exhibit carbonic anhydrase inhibition [9,10], insecticidal activity [11], antibacterial activity [12], antiviral activity [13], and anti-leishmanial activity [14], as well as other biological activities [15]. Le Questel and co-workers reported several easily synthesized 3-pyridylsulfonamide compounds that showed promise as cockroach cholinergic synaptic transmission activators [11]. Potential sulfonamide targets were identified via high-throughput virtual screening and were further evaluated in silico to determine specific target molecules to be synthesized and tested. Mohamed-Ezzat and Elgemeie have also reported a novel class of sulfonamides, some of which showed promising activity versus coronavirus 229E and NCI 60 cancer cells [13].

Sulfonamides are also useful reagents for organic synthesis. Several nickel catalysts have been reported for the formation of C–N bonds via cross-coupling. You and

check for updates

Academic Editor: Wolfram Miller

Received: 24 June 2025
Revised: 18 July 2025
Accepted: 21 July 2025
Published: 23 July 2025

Citation: Oblazny, M.; Hamaker, C.G. Structural Comparison of Three *N*-(4-Methoxyphenyl)-Nitrobenzenesulfonamide Derivatives. *Crystals* **2025**, *15*, 673. https://doi.org/10.3390/cryst15080673

Copyright: © 2025 by the authors. Licensee MDPI, Basel, Switzerland. This article is an open access article distributed under the terms and conditions of the Creative Commons Attribution (CC BY) license (https://creativecommons.org/licenses/by/4.0/).

Li reported nickel(0) catalysts for the efficient conversion of arylsulfonamides to diarylsulfonamides [16]. Xue and coworkers recently investigated nickel(II) catalyzed photochemical synthesis of aryl- and diarylsulfonamides via sulfamidation of aryl chlorides [17]. DeRatt's group used sulfonamides for the synthesis of benzomorpholines via tandem amination oxitane ring opening using palladium catalysts [18]. Several groups have also used transition metal catalysts for the *N*-alkylation of sulfonamides using alcohols. Li and coworkers used ruthenium(II) arene complexes for the selective *N*-alkylation of benzensulfonamides [19], while Anandaraj and Ramesh used palladium(II) pincer complexes for similar reactions [20]. Yu et al. also recently reported the synthesis of 1-(phenylsulfonyl)-1*H*-benzimidazoles from 2-nitrobenzenesulfonamides via tandem reactions [21].

In the solid state, sulfonamides typically primarily exhibit two hydrogen-bonding patterns, either C(4) N–H···O–S chains or $R_2^2(8)$ dimers via adjacent N–H···O–S hydrogen bonds (Figure 1) [22]. The importance of hydrogen bonding in sulfonamide crystals has long been understood [23]. In 2009, Perlovich et al. investigated the thermodynamic and structural aspects of 10 sulfonamide molecules [24]. More recently, Bolla and Nangia explored synthon hierarchy in sulfonamide cocrystals [25], and Gonnade and co-workers investigated the π–π of several sulfonamide and sulfoester derivatives [26]. Given the prevalence of the sulfonamides in bioactive molecules, an understanding of their hydrogen bonding interactions in the solid state is important.

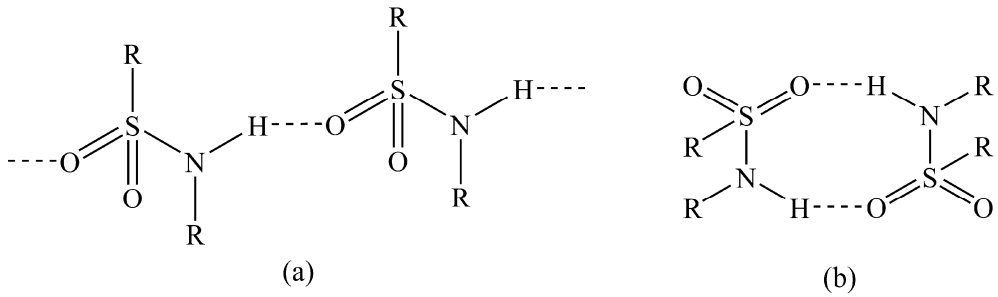

Figure 1. Common hydrogen-bonding patterns in sulfonamides: (**a**) C(4) chains; (**b**) $R_2^2(8)$ dimers.

Our group is interested in the intermolecular interactions of small molecules with strong hydrogen bonding groups [27,28] and has recently been studying the structure–property relationships in sulfonamides [14,29]. As an extension of those studies, here, we report a comparison and analysis of the crystal structures of all three isomers of *N*-(4-methoxyphenyl)-nitrobenzenesulfonamide. By systematically varying the structure of only one end of the sulfonamide molecules, we hope to observe changes in the intermolecular interactions, including hydrogen bonds, to allow us to predict the interactions in other sulfonamide molecules.

2. Materials and Methods

2.1. General Experimental Section

Starting materials were obtained from commercial sources (Sigma-Aldrich, Acros, or Alfa Aesar) and were at least 97% purity. All melting points were collected on an SRS Digimelt (Sunnyvale, CA, USA) and are uncorrected.

2.2. Synthesis and Crystallization

The synthesis of *N*-(4-methoxyphenyl)-4-nitrobenzenesulfonamide, **A**, is given as an example. 4-Nitrobenzenesulfonyl chloride (10.00 mmol, 2.2166 g) and *p*-anisidine (10.00 mmol, 1.2320 g) were added to a 250 mL Erlenmeyer flask containing 50 mL deionized water and 10 mL 1 M Na_2CO_3. The mixture was stirred on a stir plate for approximately 4 days. The product was collected by suction filtration and washed with deionized water

and isopropanol. The product was dried in oven at low heat, and the dry product weighed. Yield: 2.6466 g (85.84%). M.P.: 182–183 °C. X-ray quality crystals were grown by solvent diffusion of heptane into an acetone solution of **A**.

N-(4-methoxyphenyl)-3-nitrobenzenesulfonamide, **B**, was prepared from 3-nitrobenzenesulfonylchloride (10.01 mmol, 2.2188 g) and *p*-anisidine (10.04 mmol, 1.2366 g). Yield: 2.4580 g (79.65%). M.P.: 133–134 °C. X-ray quality crystals were grown by solvent diffusion of hexane into an acetone solution of **B**.

N-(4-methoxyphenyl)-2-nitrobenzenesulfonamide, **C**, was prepared from 2-nitrobenzenesulfonyl chloride (10.00 mmol, 2.2170 g) and *p*-anisidine (10.06 mmol, 1.2392 g). Yield: 0.5498 g (17.83%). M.P.: 85–86 °C. X-ray quality crystals were grown by solvent diffusion of hexane into a 1,2-dichloroethane solution of **C**.

2.3. Data Collection and Refinement

Data were collected on a Bruker APEX II diffractometer equipped with a CCD detector at 100(2) K using MoKα radiation (λ = 0.71073 Å). The data were processed and corrected for absorption using the Bruker (Madison, WI, USA) SAINT+ software package [30]. Structures were solved by direct methods using SHELXS-2017, and the data were refined using SHELXL-2017 [31]. All non-H atoms were refined anisotropically. Hydrogen atoms attached to carbon were assigned positions based on the geometries of their attached carbons. Hydrogen atoms bonded to oxygen and nitrogen were assigned positions based on the Fourier difference map. See Table 1 for final refinement parameters. Figures were made using ORTEP3 [32], Mercury [33], and CrystalExplorer [34].

Table 1. Data collection parameters.

Compound	A (*p*-NO_2)	B (*m*-NO_2)	C (*o*-NO_2)
CCDC Deposit No.	2467049	2467050	2467051
Chemical formula	$C_{13}H_{12}N_2O_5S$	$C_{13}H_{12}N_2O_5S$	$C_{13}H_{12}N_2O_5S$
M_r	308.31	308.31	308.31
Crystal system, space group	Monoclinic, *Cc*	Monoclinic, $P2_1/c$	Monoclinic, $P2_1/c$
Temperature (K)	100 (2)	100 (2)	100 (2)
a, *b*, *c* (Å)	5.1710 (4) 12.9028 (10) 19.7324 (15)	20.5686 (7) 5.1731 (2) 13.0803 (5)	12.0195 (7) 7.2684 (4) 15.0297 (8)
β (°)	94.420 (4)	107.7598 (16)	91.529 (3)
V (Å^3)	1312.64 (8)	1325.46 (9)	1312.27 (13)
Z	4	4	4
Radiation type	Mo K_α	Mo K_α	Mo K_α
μ (mm^{-1})	0.271	0.269	0.271
Crystal size (mm)	0.28 × 0.20 × 0.13	0.39 × 0.32 × 0.20	0.31 × 0.18 × 0.10
Diffractometer	Bruker *APEX*-II CCD		
Absorption correction	Multi-scan *SADABS*		
T_{min}, T_{max}	0.70, 0.75	0.90, 0.95	0.92, 0.97
No. measured, independent, and observed [$I > 2\sigma(I)$] reflections	17529, 2667, 2661	36710, 2815, 2749	38370, 2880, 2687
R_{int}	0.020	0.017	0.024
$(\sin\theta/\lambda)_{max}$ (Å^{-1})	0.625	0.633	0.641
$R[F^2 > 2\sigma(F^2)]$, $wR(F^2)$, *S*	0.0291, 0.0874, 1.173	0.0277, 0.0750, 1.052	0.0277, 0.0729, 1.065
No. of reflections	2667	2815	2880
No. of parameters	194	194	194
H-atom treatment	H atoms treated by a mixture of independent and constrained refinement		
Δr_{max}, Δr_{min} (e Å^{-3})	0.50, −0.32	0.48, −0.45	0.41, −0.41

Computer programs: Bruker APEX2 [25], Bruker SAINT [25], SHELXS97 [26], and SHELXL97 [26].

3. Results and Discussion

3.1. Synthesis

The sulfonamides were all prepared by stirring solutions of *p*-anisidine and X-nitrobenzenesulfonyl chloride in aqueous sodium carbonate at room temperature. The products were collected via suction filtration. All products matched previous reports of the compounds in the literature [35,36].

3.2. Crystal Structures

Figure 2 shows the ORTEP diagrams of compounds **A**, **B**, and **C**. All three show bond distances and angles in the range of other *N*-(4-methoxyphenyl)-sulfonamides [37] (Tables 2 and 3), and all three have very similar overall structures. A search of the Cambridge Structural Database (CSD) for *N*-(4-methoxyphenyl)-sulfonamides resulted in 23 structures. The average bond lengths [S–C: 1.766 (9) Å; S–N: 1.633 (9) Å; N=C: 1.441 (6) Å] are all very similar to the distances in **A**, **B**, and **C**. Examining the bond angles, the C1–S1–N1 angles in all three are smaller than the CSD average of 107.4 (13)°. In fact, all three are smaller than the smallest C–S–N angle in the previous 23 structures, which is 105.8 (2)° for entry CEDCIZ, *N*-(4-methoxyphenyl)-4-iodobenzenesulfonamide [38]. The S1–N1–C7 angles for **A** and **B** fall within the range of the 23 (116.812–120.376°), while for **C**, the angle is now the smallest reported for all *N*-(4-methoxyphenyl)-sulfonamides, at 115.49 (8)°. The CSD search found a range of 117.903–120.532° for the O–S–O angle. Of the three molecules reported in this study, **C** falls well within the range at 118.98 (6)°, **A** is near the maximum at 120.45 (14)°, and **C** is now the largest O–S–O angle at 120.66 (5)°, though not by a significant amount.

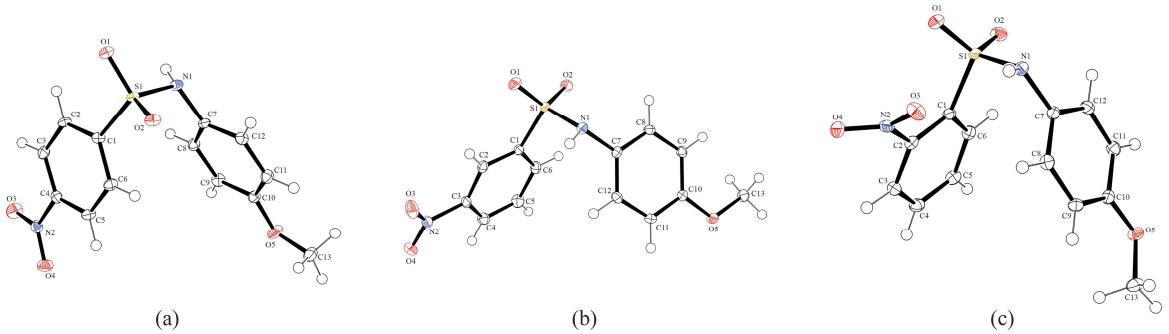

(a) (b) (c)

Figure 2. Molecular structures of compounds (**a**) **A**, (**b**) **B**, and (**c**) **C**, showing the atom numbering schemes. The thermal ellipsoids are drawn at a 50% probability level, with hydrogen atoms shown as spheres of arbitrary size.

Table 2. Selected bond distances (Å).

Bond	A (*p*-NO_2)	B (*m*-NO_2)	C (*o*-NO_2)
S1–C1	1.770 (3)	1.7664 (12)	1.7871 (12)
S1–N1	1.646 (3)	1.6450 (10)	1.6426 (11)
N1–C7	1.450 (4)	1.4415 (14)	1.4467 (15)

Table 3. Selected bond and torsion angles (°).

Bond	A (*p*-NO_2)	B (*m*-NO_2)	C (*o*-NO_2)
C1–S1–N1	105.43 (15)	105.00 (5)	104.97 (5)
S1–N1–C7	116.9 (2)	119.00 (8)	115.49 (8)
O1–S1–O2	120.45 (14)	120.66 (5)	118.98 (6)
C1–S1–N1–C7	–58.6 (3)	66.56 (3)	41.78 (10)

Hydrogen bonding interactions for all three molecules are given in Tables 4–6. There are only two bond angles that are significantly different in any of the three molecules. First is the S1–N1–C7 angle, which is largest in **B** [119.00 (8)°] and smallest in **C** [115.9 (8)°], with **A** [116.9 (2)°] in between the other two. The other is the O1–S1–O2 angle, which is smaller in **C** [118.98 (6)°] than in **A** [120.45 (14)°] or **B** [120.66 (5)°], which are very similar. Additionally, the C1–S1–N1–C7 torsion angle is quite different in all three, giving rise to different relative orientations for the phenyl rings in the three molecules. Figure 3a shows an overlay, prepared using Mercury, of molecules **A**, **B**, and **C** using C7, C9, C11, and O5 as the anchoring atoms, looking down the N1–C7 bond [33]. With all three methoxy groups oriented the same direction, you can see the effect of the different C1–S1–N1–C7 torsion angles for the three molecules. Figure 3b shows an alternative overlay of the three molecules along the N1–C7 bond, anchored using S1, N1, and H1. In this orientation, the negative torsion angle of **A**, −58.6 (3)°, is compared to the positive torsion angles of **B**, +66.56 (3)°, and **C**, +41.78 (10)°. All three torsion angles fall within the range of the other *N*-(4-methoxyphenyl)-sulfonamides [37] in the CSD search, where the 23 molecules ranged from −68.704° to +71.3°.

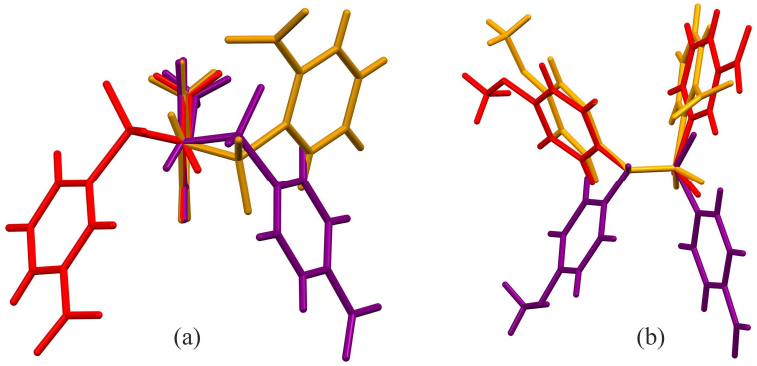

Figure 3. Capped stick overlay of compounds **A** (purple), **B** (red), and **C** (gold) visualized using Mercury [33], with (**a**) viewed down the N1–C7 bond anchored via C7, C9, C11, and O5, and (**b**) viewed along the N1–C7 bond with S1, N1, and H1 the anchoring atoms.

The third difference in the molecules is the angle between the planes formed by the C1–C6 ring and the nitro group (N2, O3, O4). In molecules **A** [8.1 (5)°] and **B** [7.83 (19)°], they are nearly coplanar, while in **C** [47.35 (7)°], the nitro is twisted away from the benzene ring due to steric interference from the sulfonamide group.

Table 4. Hydrogen bonding geometry (Å, °) for **A**.

D–H···A	*D*–H	H···A	*D*···A	*D*–H···A
C5–H5···O1 ^{i}	0.95	2.43	3.144 (4)	132
C2–H2···O4 ^{ii}	0.95	2.52	3.294 (4)	139
C11–H11···O3 ^{iii}	0.95	2.50	3.414 (4)	161
N1–H1···O2 ^{iv}	0.89 (6)	2.25 (6)	3.089 (4)	156 (5)
C13–H13A···O4 ^{v}	0.98	2.56	3.352 (5)	138

Symmetry codes: (*i*) $x + ½, y - ½, z$; (*ii*) $x - ½, y + ½, z$; (*iii*) $x + 1, -y, z - ½$; (*iv*) $x - 1, y, z$; (*v*) $x + ½, -y - ½, z - ½$.

Table 5. Hydrogen bonding geometry (Å, °) for **B**.

D–H···A	*D*–H	H···A	*D*···A	*D*–H···A
C13–H13*A*···O5 ^{i}	0.98	2.60	34703 (15)	148
C4–H4···O4 ^{ii}	0.95	2.42	3.2965 (16)	153
N1–H1···O2 ^{iii}	0.856 (18)	2.176 (19)	3.0127 (14)	165.5 (16)

Symmetry codes: $-y + 1, -z + 1$; (*ii*) $-x, -y + 2, -z$; (*iii*) $x, y + 1, z$.

Table 6. Hydrogen bonding geometry (Å, °) for **C**.

D–H···A	*D*–H	H···A	*D*···A	*D*–H···A
N1–H1···O5 ^{i}	0.826 (19)	2.281 (19)	3.0534 (14)	155.8 (16)
N1–H1···O3	0.826 (19)	2.524 (18)	3.0612 (14)	123.8 (15)
C13–H13*A*···O2 ^{ii}	0.98	2.47	3.2891 (16)	141

Symmetry codes: (*i*) $x, y-1, z$; (*ii*) $x, -y+3/2, z+½$.

Compound **A** exhibits several intermolecular contacts in the crystal structure (Figure 4). First is the formation of C(4) chains (Figure 4a) along the *a*-axis via N1–H1···O2 hydrogen bonds (pink). The chains are linked together into a three-dimensional network via $R_2^2(10)$ rings involving C–H···O interactions between the C5 on the nitrobenzene ring and sulfonamide oxygen O1 (orange) and C2 with the nitro oxygen O4 (green). Additionally, there is a C11–H11···O3 interaction (purple), generating C(12) chains, as well as a C11–H13A···O4 interactions (blue), yielding C(15) chains. Alternatively, the two chain interactions combine to form large $R_4^4(30)$ rings, which are assembled via the previously described $R_2^2(10)$ rings into a three-dimensional structure (Figure 4d). Compound A also exhibits an S=O···N_{nitro} contact, where the O···N distance is 2.991 (4) Å, which is 0.169 Å shorter than the sum of their van der Waals radii [39] (Figure 4b).

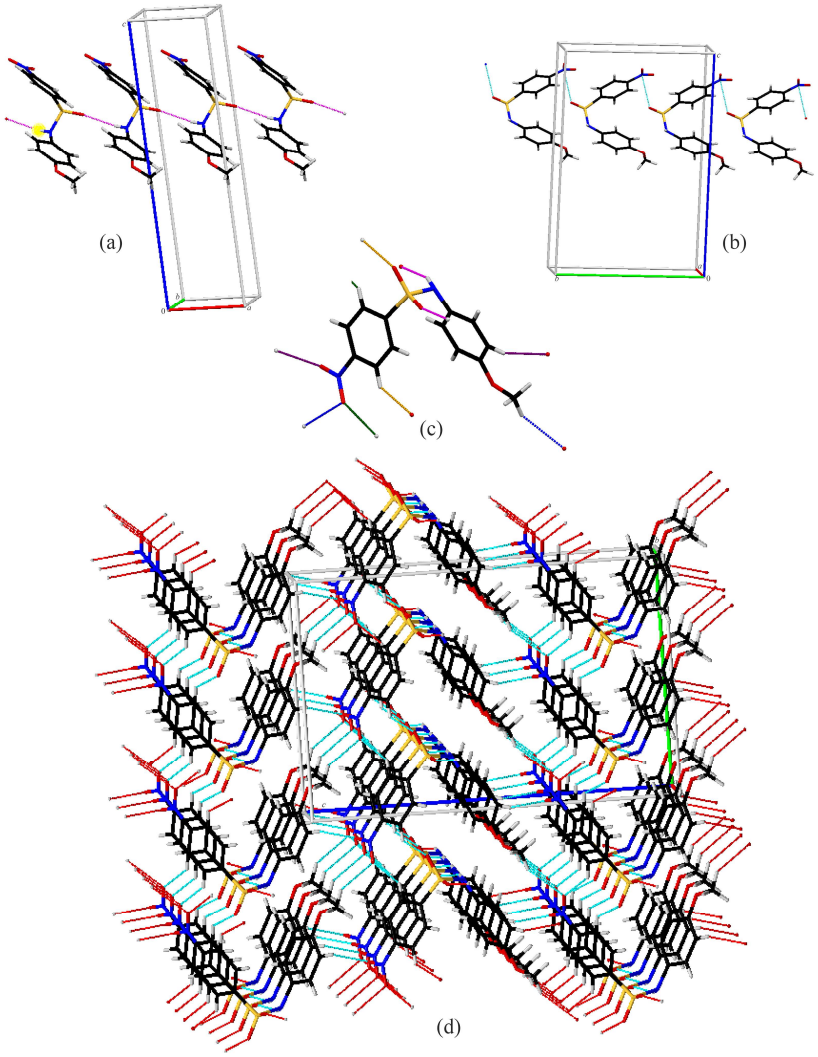

Figure 4. Capped stick diagrams of intermolecular contacts in **A**. (**a**) N1–H1···O2 hydrogen bond chains; (**b**) S=O···N_{nitro} contact chains; (**c**) single molecule showing each interaction; (**d**) three-dimensional packing.

Figure 5 shows the intermolecular contacts in Compound **B**. Molecules of **B** form C(4) chains along the *b*-axis via N1–H1···O2 hydrogen bonds (pink). The chains are linked together by $R_2^2(10)$ C4–H4···O4 interactions (green), forming one-dimensional ladders running along the *b*-axis. The combination of the chains gives rise to $R_4^4(30)$ rings. Combined with C13–H13A···O5 interactions (orange), they make up the rungs of a *Stairway to Heaven* (Figure 5b). Compound **B** also exhibits a nitro O···N contact, with a distance of 2.883(2) Å, which is 0.277Å less than the sum of the van der Waals radii of nitrogen and oxygen [39] (Figure 5c). These O···N contacts connect the stairways together, extending the structure into a three-dimensional network.

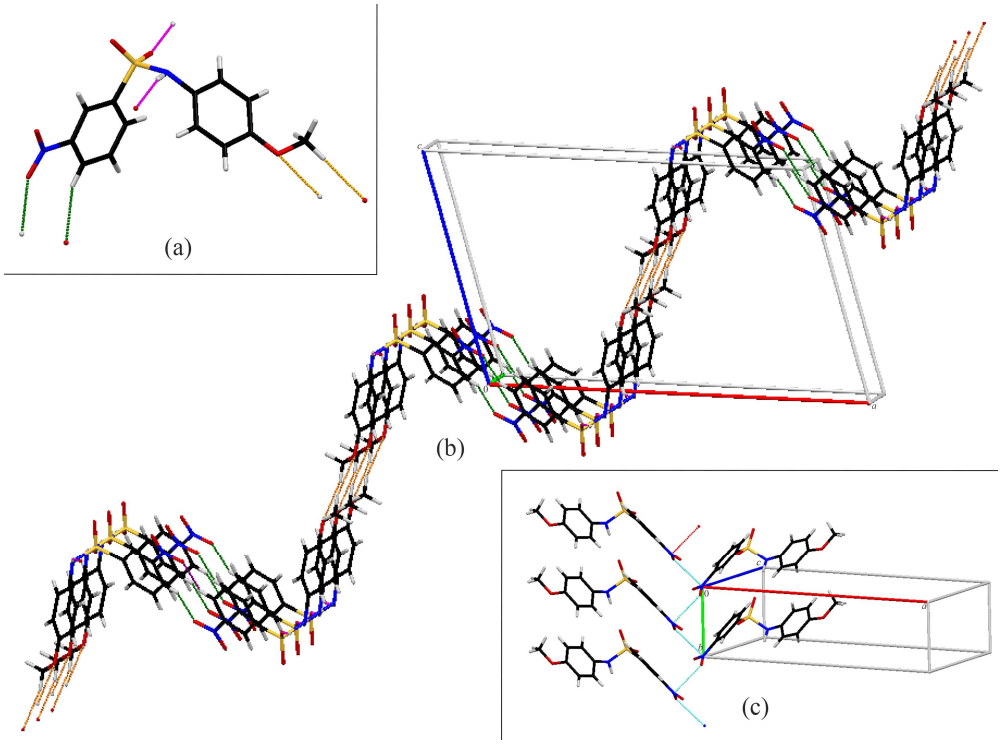

Figure 5. Capped stick diagrams of intermolecular contacts in **B**. (**a**) Single molecule showing each interaction; (**b**) three-dimensional ladder; (**c**) nitro N2···O4 contact.

Molecule **C** has the only intramolecular hydrogen bonding interaction. The intermolecular interactions for compound **C** are shown in Figure 6. **C** also forms chains along the *b*-axis via N–H···O (Figure 6c) hydrogen bonds (pink). However, the acceptor oxygen is the methoxy oxygen of the neighboring molecule, not a nitro or sulfonamide oxygen, resulting in C(7) chains. This is likely due to the nitro group not being coplanar to the attached benzene ring. The chains are linked together into two-dimensional sheets via C13–H13···O2 interactions (orange) (Figure 6c). Additionally, there are nitro–nitro interactions between molecules with an N2···O4 distance of 2.857 (1) Å, approximately 0.303Å shorter than the van der Waals sum [39], forming $R_2^2(4)$ dimers (Figure 6c).

Examining the melting points of the three molecules, **A** has the highest of the three, 182–183°. Compound **A** has traditional, strong, and directional N–H···O sulfonamide C(4) hydrogen bonds along with an S=O···N_{nitro} contact and four C–H···O contacts, more than either **B** or **C**, resulting in a rigid three-dimensional network (Figure 4d). Compound **B** has the next highest melting point of the three, 133–134 °C. While **B** also contains strong, directional N–H···O sulfonamide C(4) hydrogen bonds, there are only two C–H···O contacts, along with the nitro O···N contact. The stairway sheets are only connected by these O···N contacts and, along with the fewer C–H···O contacts, result in a lower melting point. Of the three, **C** has the lowest melting point, 85–86 °C. While **C** also has an N–H···O

hydrogen bond, the acceptor is the methoxy oxygen, which is expected to have a smaller negative charge than the sulfonamide oxygens, resulting in a weaker hydrogen bond interaction compared to **A** and **B**. The two-dimensional sheets of **C** are held together by relatively weak, by comparison, π–π contacts, resulting overall in a lower melting point than either **A** or **B**.

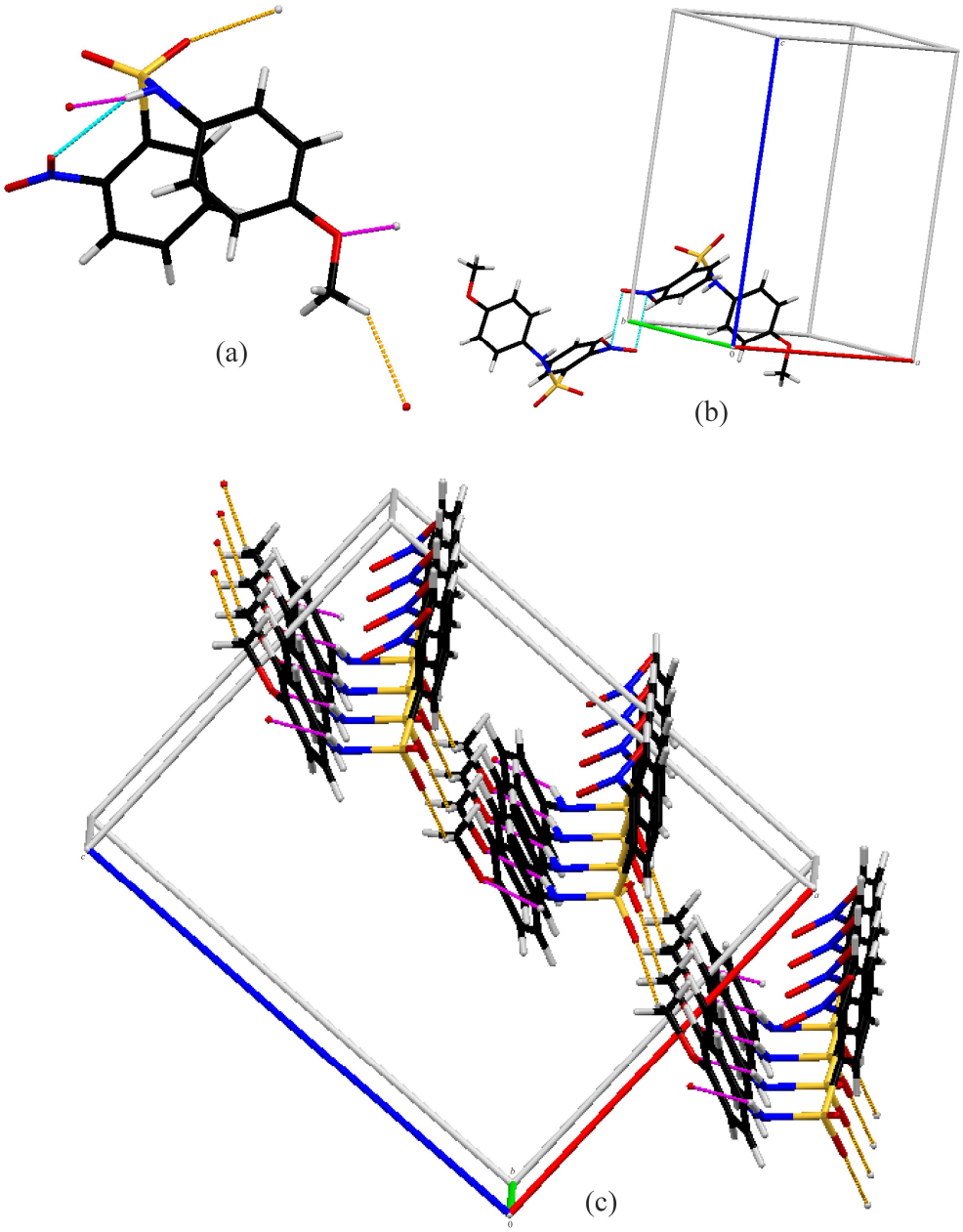

Figure 6. Capped stick diagrams of intermolecular contacts in **C**. (**a**) Single molecule showing each interaction; (**b**) nitro···nitro dimer; (**c**) three-dimensional sheets.

3.3. Hirshfeld Analysis

Examination of the Hirshfeld surface plots for the molecules (Figure 7) reveals several similarities. Looking at the surfaces, molecules **A** and **C** are more compact than **B**. All three show short contacts, as indicated by the red regions of the Hirshfeld surfaces. Of note, the short contacts on the surface are mostly between hydrogen and oxygen atoms, although the Hirshfeld surfaces are helpful for finding non-hydrogen bonding interactions. In molecule **A**, the S=O···N_{nitro} contact is evident (O1···N2); in **B**, nitro O3···N2 contact is evident; in **C**, the nitro-nitro contact is indicated by two neighboring red spots on the Hirshfeld surface.

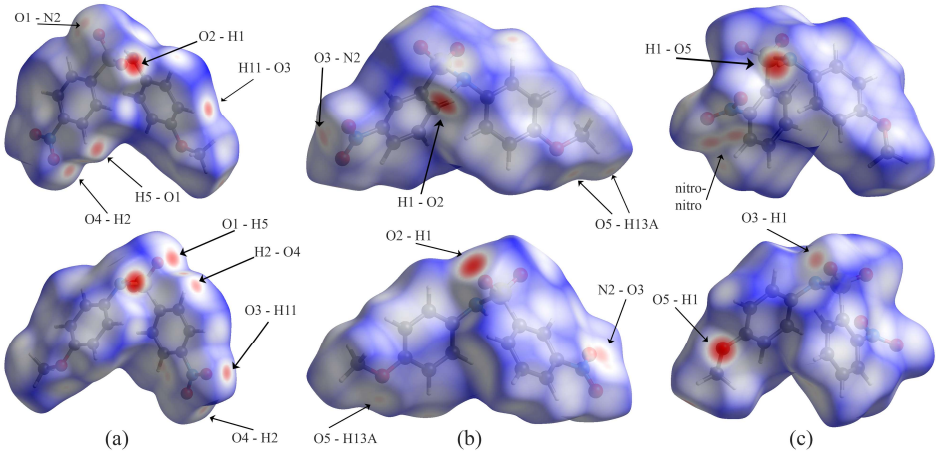

Figure 7. Hirshfeld plots for compounds (**a**) **A**, (**b**) **B**, and (**c**) **C**, showing two faces for each molecule.

For all three structures, the most prevalent contacts are H···O, followed by H···H and H···C. The only other contacts to make up more than 5% in any of the structures are C···O contacts, which represent 5.7% in **A**, 8.9% in **B**, and 4.7% in **C**. Looking at the fingerprint plots for **A** (Figure 8), the contacts are relatively compact. The H···O contacts show the typical hydrogen-bonding "fangs", while the H···H are generally distributed throughout the plot, with a sharp point between the hydrogen-bonding fangs corresponding to the shortest contact between H2 and H5 of neighboring molecules. The H···C interactions are generally longer than the other hydrogen contacts. In molecule **B** (Figure 9), the H···O plot shows the typical fangs, while the H···H contacts culminate in a much broader peak. The H···C contacts show wings on the outer edges of the plot, as well as some shorter H···C contacts compared to **A** and **C**, indicating shorter and stronger interactions. The fingerprint plots for molecule **C** (Figure 10) also show the H···O fangs as well as the H···H point between the fangs, indicating the shortest H···H contact between H8 and H13A. The major difference between **C** and the other two molecules is seen in the H···C contacts, which are more spread out.

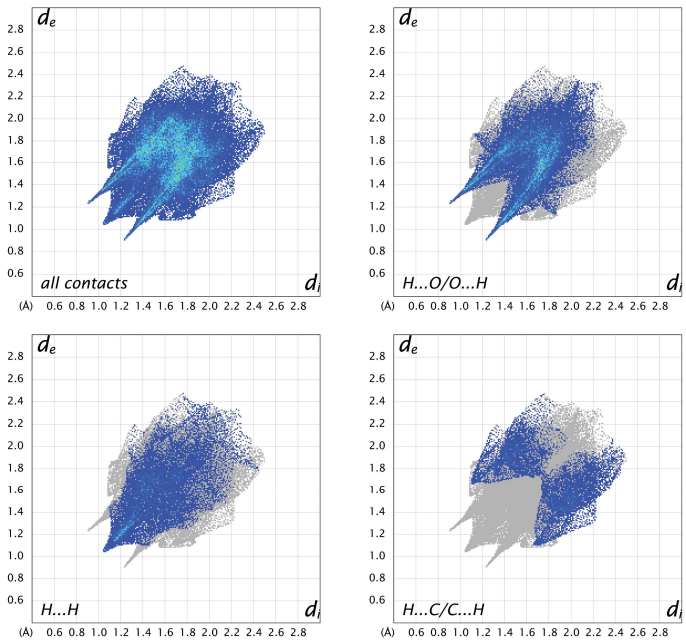

Figure 8. Two-dimensional fingerprint plots for all interactions and important (O···H, H···H, and C···H) interatomic contacts in **A**.

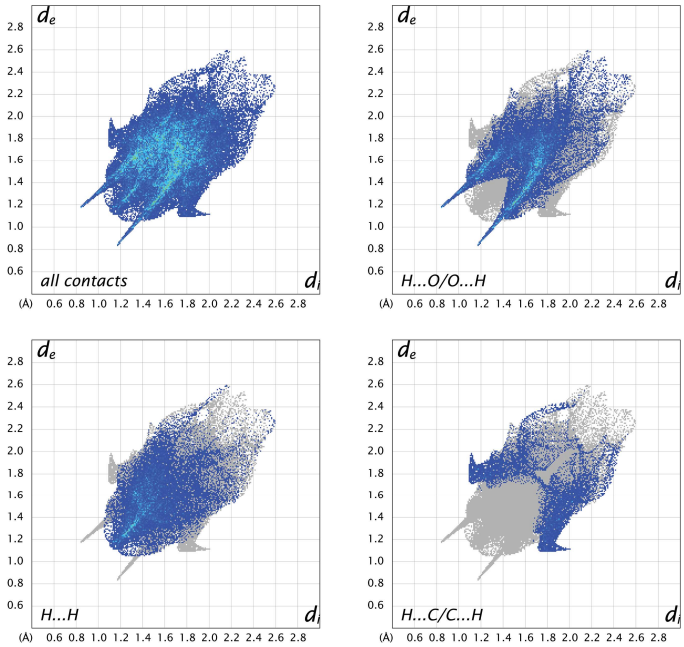

Figure 9. Two-dimensional fingerprint plots for all interactions and important (O···H, H···H, and C···H) interatomic contacts in **B**.

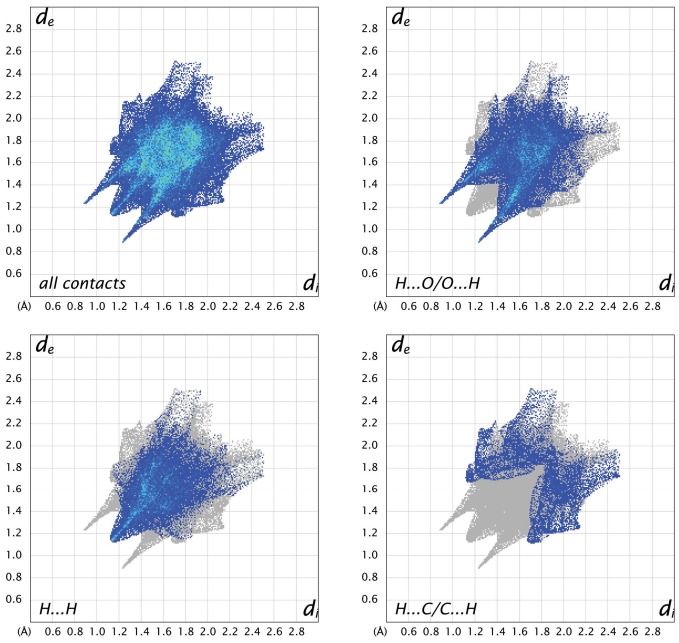

Figure 10. Two-dimensional fingerprint plots for all interactions and important (O···H, H···H, and C···H) interatomic contacts in **C**.

Of the three structures, only **C** shows any π···π contacts, which can be seen in looking at the percentage of C···C contacts in each molecule (3.3% in **C**, 0% in **A**, 0.3% in **B**). The π···π contact can also be seen in the shape index plot for **C** (Figure 11), indicated by the adjacent diamond shapes on the surface of the methoxy phenyl ring. The Cg···Cg distance between the two methoxyphenyl rings is 3.7351 (7) Å.

As can be seen in Figure 7, all three molecules have a relatively compact overall shape in the crystal structures. While molecule **B** appears less compact than **A** or **C**, the molecular volumes of the molecules calculated using MoloVol [40] are very similar: 265.1 Å^3 for **A**, 264.8 Å^3 for **B**, and 265.7 Å^3 for **C**. Since all three molecules have $Z = 4$, their unit cell volumes are also very similar (Table 1). While the C1–S1–N1–C7 torsion angles (Table 3) are

all very different, the angle between the two aromatic rings is similar in all three molecules: 30.51 (14)° in **A**, 41.05 (5)° in **B**, and 41.06 (5)° in **C**. Focusing on the sulfonamide nitrogen atom in the structures, it is only slightly pyramidalized. The displacement of the N1 atom from the plane defined by S1–H1–C7 is remarkably similar in all three and quite small: 0.32 (3) Å for **A**, 0.323 (8) Å for **B**, and 0.325 (9) for **C**. The one significant difference in **B** compared to **A** and **C** is the S1–N1–C7 angle, which is larger in **B**, leading to a less compact overall structure.

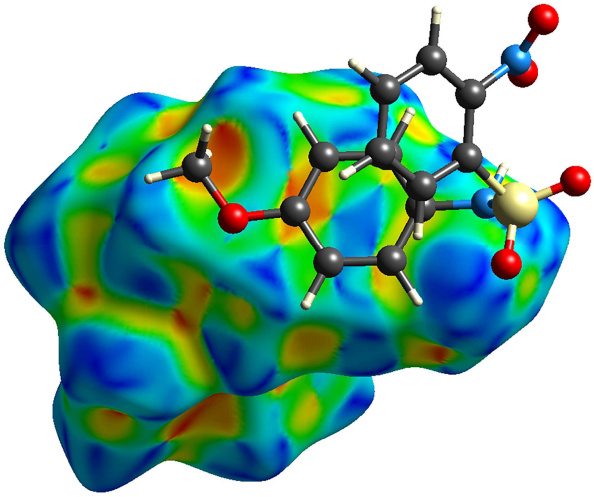

Figure 11. Shape index plot for compound **C** showing the π···π interaction between molecules.

4. Conclusions

In an effort to understand the effects of substitution geometry on the crystal structures of sulfonamide derivatives, the single crystal X-ray structures of all three geometric isomers of *N*-(4-methoxyphenyl)-X-nitrobenzenesulfonamide were determined, and their intermolecular interactions investigated. Despite the similar structures of all three molecules, they all feature quite different interactions in the crystalline state. In molecules **A** and **B**, the sulfonamide hydrogen forms C(4) hydrogen bonds with sulfonamide oxygens. However, in molecule **C**, there is an intramolecular N–H···O hydrogen bond, and the intermolecular hydrogen bond acceptor is the methoxy oxygen, forming C(7) chains. Overall, it appears the position of the nitro group on the sulfonamide benzene ring has significant effects on the interactions between molecules in the crystals. The position of the nitro group leads to different packing between the molecules, resulting in the different orientations of the aromatic rings relative to each other in the three molecules, which are manifested in the different torsion angles seen. These orientations lead to the variation in the intermolecular interactions and three-dimensional packing of the molecules. The structures of the three molecules in this study did not reveal any obvious patterns in the intermolecular interactions within the series. Therefore, further studies are underway to better understand the factors that influence the hydrogen bonding and packing patterns of diarylsulfonamide and related molecules.

Supplementary Materials: The following supporting information can be downloaded at: https://www.mdpi.com/article/10.3390/cryst15080673/s1. CCDC 2467049–2467051 contain the supplementary crystallographic data for this paper. These data can be obtained free of charge from The Cambridge Crystallographic Data Centre via www.ccdc.cam.ac.uk/structures.

Author Contributions: Methodology and investigation, M.O. and C.G.H.; preliminary writing, M.O.; writing—review and editing, C.G.H.; supervision and funding acquisition, C.G.H. All authors have read and agreed to the published version of the manuscript.

Funding: C.G.H. wishes to thank the Illinois State University Chemistry Department for financial support. We also thank the NSF (Grant no. CHE-1039689) for funding the X-ray diffractometer.

Data Availability Statement: The original contributions presented in the study are included in the article/Supplementary Materials. Further inquiries can be directed to the corresponding author.

Conflicts of Interest: The authors declare no conflicts of interest.

References

1. Lesch, J.E. *The First Miricle Drugs How the Sulfa Drugs Transformed Medicine*; Oxford University Press: Oxford, UK, 2007; pp. 51–67.
2. Sulfonamides. Available online: https://my.clevelandclinic.org/health/treatments/sulfonamides (accessed on 18 June 2025).
3. Zessel, K.; Mohring, S.; Hamscher, G.; Kietzmann, K.; Stahl, J. Biocompatibility and antibacterial activity of photolytic products of sulfonamides. *Chemosphere* **2014**, *100*, 167–174. [CrossRef]
4. Liu, W.; Chen, J.; Su, W. Recent Advances in the Synthesis of Sulfonamides Intermediates. *Pharmaceut. Fronts* **2024**, *6*, e355–e381. [CrossRef]
5. Elsayad, K.A.; Elmasry, G.F.; Mahmoud, S.T.; Awadullah, F.M. Sulfonamides as anticancer agents: A brief review on sulfonamide derivatives as inhibitors of various proteins overexpressed in cancer. *Bioorg. Chem.* **2024**, *147*, 107409. [CrossRef] [PubMed]
6. Wan, Y.; Fang, G.; Chen, H.; Deng, X.; Tang, Z. Sulfonamide derivatives as potential anti-cancer agents and their SARs elucidation. *Eur. J. Med. Chem.* **2021**, *226*, 113837. [CrossRef] [PubMed]
7. Ortiz, M.A.; Michaels, H.; Molina, B.; Toenjes, S.; Davis, J.; Marconi, G.D.; Hecht, D.; Gustafson, J.L.; Piedrafita, F.J.; Nefzi, A. Discovery of cyclic guanidine-linked sulfonamides as inhibitors of LMTK3 kinase. *Bioorg. Med. Chem. Let.* **2020**, *30*, 127108. [CrossRef]
8. Xu, Y.; Zhang, H.; Lit, L.C.; Grothey, A.; Athanasiadou, M.; Kiritsi, M.; Lombardo, Y.; Frampton, A.E.; Green, A.R.; Ellis, I.O.; et al. The kinase LMTK3 promotes invasion in breast cancer through GRB2-mediated induction of integrin β_1. *Sci. Signal.* **2014**, *7*, ra58. [CrossRef]
9. Szafrański, K.; Sławiński, J.; Kawiak, A.; Chojnacki, J.; Kosno, M.; Ammara, A.; Supuran, C.T. 4-Substituted Pyridine-3-Sulfonamides as Carbonic Anhydrase Inhibitors Modified by Click Tailing: Synthesis, Activity, and Docking Studies. *Int. J. Mol. Sci.* **2025**, *26*, 3817. [CrossRef]
10. Fadaly, W.A.A.; Nemr, M.T.M.; Abd El-Hameed, A.M.; Giovannuzzi, S.; Alkabbani, M.A.; Hefina, M.M.; Nocentini, A.; Mohamed, M.F.A.; Supuran, C.T.; Eldehna, W.M.; et al. Novel benzenesulfonamide derivatives linked to diaryl pyrazole tail as potential carbonic anhydrase II/VII inhibitors with anti-epileptic activity. *Eur. J. Med. Chem.* **2025**, *291*, 117619. [CrossRef]
11. Selvam, B.; Landagaray, E.; Cartereau, E.A.; Laurent, A.D.; Graton, J.; Lebreton, J.; Thany, S.H.; Mathé-Allainmat, M.; Le Questel, J.-Y. Identification of sulfonamide compounds active on the insect nervous system: Molecular modeling, synthesis and biological evaluation. *Bioorg. Med. Chem. Lett.* **2023**, *80*, 129124. [CrossRef]
12. Gaffer, H.E.; Mahmoud, S.A.; El-Sedik, M.S.; Aysha, T.; Abdel-Rhman, M.H.; Abdel-Latif, E. Synthesis, molecular modelling, and antibacterial evaluation of new sulfonamide-dyes based pyrrole compounds. *Sci. Rep.* **2024**, *14*, 10973. [CrossRef]
13. Mohamed-Ezzat, R.A.; Elgemeie, G.H. Novel synthesis of the first new class of triazine sulfonamide thioglycosides and the evaluation of their anti-tumor and anti-viral activities against human coronavirus. *Nucleosides Nucleotides Nucleic* **2024**, *43*, 1511–1528. [CrossRef]
14. Li, E.W.; Katinas, J.; Jones, M.A.; Hamaker, C.G. Structural characterization of naphthalene sulfonamides and a sulfonate ester and their in vitro efficacy against *Leishmania tarentolae* promastigotes. *New J. Chem.* **2021**, *45*, 4791–4801. [CrossRef]
15. Ochu, R.C.; Okoro, U.C.; Conradie, J.; Ugwu, D.I. New antibacterial, antifungal and antioxidant agents bearing sulfonamide. *Eur. J. Med. Chem. Rep.* **2024**, *10*, 100136. [CrossRef]
16. You, T.; Li, J. Ni(cod)(duroquinone)-Catalyzed C−N Cross-Coupling for the Synthesis of *N*,*N*-Diarylsulfonamides. *Org. Lett.* **2022**, *24*, 6642–6646. [CrossRef] [PubMed]
17. Song, G.; Song, J.; Dong, J.; Li, G.; Fan, J.; Xue, D. Ni-Catalyzed Photochemial Sulfamidation of Aryl Chlorides with Soluble Organic Amine as Base. *Organometallics* **2024**, *43*, 1706–1712. [CrossRef]
18. Deratt, L.G.; Wang, C.Y.; Kuduk, S.D. Tandem Amination/Oxetane Ring Opening toward Benzomorpholines. *J. Org. Chem.* **2021**, *86*, 17482–17486. [CrossRef]
19. Shen, L.; Wu, X.; Shi, L.; Xu, X.; Zhang, J.; Li, F. Selective N-Alkylation of Aminobenzenesulfonamides with Alcohols for the Synthesis of Amino-(N-Alkyl)benzenesulfonamides Catalyzed by a Metal-Ligand Bifunctional Ruthenium Catalyst. *J. Org. Chem.* **2024**, *89*, 8397–8406. [CrossRef] [PubMed]
20. Anandaraj, P.; Ramesh, R. *N*-alkylation of benzamides/sulfonamides using alcohols via borrowing hydrogen approach by well-defined Pd(II) pincer complexes. *Appl. Organomet. Chem.* **2023**, *37*, e7228. [CrossRef]

21. Yu, X.; Ma, Z.; Zhu, W.; Liu, H.; Zhang, Z.; Liu, Y.; Zhang, M.; Zhao, J.; Zhang, P.; Xia, C. Tandem Reduction, Ammonolysis, Condensation, and Deamination Reaction for Synthesis of Benzothiadiazines and 1-(Phenylsulfonyl)-1H-benzimidazoles. *J. Org. Chem.* **2022**, *87*, 14738–14752. [CrossRef]
22. Etter, M.C.; MacDonald, J.C.; Bernstein, J. Graph-set analysis of hydrogen-bond patterns in organic crystals. *Acta Crystallogr.* **1990**, *B46*, 256–262. [CrossRef]
23. Asmond, D.A.; Grant, D.J.W. Hydrogen bonding in sulfonamides. *J. Pharm. Sci.* **2001**, *90*, 2058–2077. [CrossRef] [PubMed]
24. Perlovich, G.L.; Tkachev, V.V.; Strakhova, N.N.; Kazachenko, V.P.; Volkova, T.V.; Surov, O.V.; Schaper, K.-J.; Raevsky, O.A. Thermodynamic and structural aspects of sulfonamide crystals and solutions. *J. Pharm. Sci.* **2009**, *98*, 4738–4755. [CrossRef] [PubMed]
25. Bolla, G.; Nangia, A. Supramolecular synthon hierarchy in sulfonamide cocrystals with *syn*-amides and *N*-oxides. *IUCrJ* **2019**, *6*, 751–760. [CrossRef]
26. Shaikh, S.R.; Gawade, R.L.; Dabke, N.B.; Dahs, S.R.; Vanka, K.; Gonnade, R.G. Crystal engineering for intramolecular π–π stacking: Effect of substitution of electron-donating and electron-withdrawing groups on the molecular geometry in conformationally flexible Sulfoesters and sulfonamides. *CrystEngComm* **2024**, *26*, 3557–3573. [CrossRef]
27. Goettler, P.E.; Hamaker, C.G. Crystal structure analysis of two 4-nitro-*N*-methylaniline derivatives. *J. Chem. Cryst.* **2022**, *52*, 251–259. [CrossRef]
28. Hamaker, C.G.; Oberts, B.P. Synthesis and crystal structures of the bis-Schiff bases of 2-(methylthio)aniline with isophthaldehyde, terephthaldehyde, and para-diacetylbenzene. *J. Chem. Cryst.* **2006**, *36*, 735–742. [CrossRef]
29. Shang, H.H.; Zelaya, Z.Z.; Hamaker, C.G.; Jones, M.A. Inhibitory Effects of Sulfur Derivatives on *Leishmania tarentolae* Cell Viability and Secreted Acid Phosphatase In Vitro. *Microorganisms* **2024**, *12*, 2641. [CrossRef]
30. *SAINT*; Bruker AXS Inc.: Madison, WI, USA, 2015.
31. Sheldrick, G.M. Crystal Structure Refinement with SHELXL. *Acta Crystallogr.* **2015**, *C71*, 3–8.
32. Farrugia, L.J. WinGX and ORTEP for Windows: An Update. *J. Appl. Crystallogr.* **2012**, *45*, 849–854. [CrossRef]
33. Macrae, C.F.; Sovago, I.; Cottrell, S.J.; Galek, P.T.A.; McCabe, P.; Pidcock, E.; Platings, M.; Shields, G.P.; Stevens, J.S.; Towler, M.; et al. Mercury 4.0: From visualization to analysis, design and prediction. *J. Appl. Crystallogr.* **2020**, *53*, 226–235. [CrossRef]
34. Turner, M.J.; McKinnon, J.J.; Wolff, S.K.; Grimwood, D.J.; Spackman, P.R.; Jayatilaka, D.; Spackman, M.A. *Crystal Explorer 17*; The University of Western Australia: Perth, Australia, 2017.
35. Mansfeld, M.; Pařík, P.; Ludwig, M. Effect of Para Substitution on Dissociation of *N*-Phenylbenzenesulfonamides. *Collect. Czech. Chem. Commun.* **2004**, *69*, 1479–1490. [CrossRef]
36. Formen, J.S.S.K.; Wolf, C. Optical Relay Sensing of Cryptochiral Alcohols Displaying α-, β-, γ- and δ-Stereocenters or Chirality by Virtue of Isotopic Substitution. *Angew. Chem. Int. Ed.* **2024**, *63*, e202409790. [CrossRef]
37. Groom, C.R.; Bruno, I.J.; Lightfoot, M.P.; Ward, S.C. The Cambridge Structural Database. *Acta Crystallogr.* **2016**, *B72*, 171–179. [CrossRef]
38. Gelbrich, T.; Threlfall, T.L.; Hursthouse, M.B. Eight isostructural 4,4′-disubstituted N-phenyl benzene sulfonamides. *Acta Crystallogr.* **2012**, *C68*, o421–o426.
39. Alvarez, S. A cartography of the van der Waals territories. *Dalton Trans.* **2013**, *42*, 8617–8636. [CrossRef]
40. Maglic, J.B.; Levendomme, R. MoloVol: An easy-to-use program for analyzing cavities, volumes and surface areas of chemical structures. *J. Appl. Crystallogr.* **2022**, *55*, 1033–1044. [CrossRef]

Disclaimer/Publisher's Note: The statements, opinions and data contained in all publications are solely those of the individual author(s) and contributor(s) and not of MDPI and/or the editor(s). MDPI and/or the editor(s) disclaim responsibility for any injury to people or property resulting from any ideas, methods, instructions or products referred to in the content.